

Article

Cul-De-Sac of the Spatial Image of Proton Interactions

Igor Dremin

Lebedev Physics Institute, Moscow 119991, Russia; dremin@lpi.ru

Received: 11 December 2018; Accepted: 28 January 2019; Published: 30 January 2019



Abstract: The unitarity condition in the impact parameter space is used to obtain some information about the shape of the interaction region of colliding protons. It is shown that, strictly speaking, a reliable conclusion can be gained only if the behavior of the elastic scattering amplitude (especially, its imaginary part) at all transferred momenta is known. This information is currently impossible to obtain from experimentation. In practice, several assumptions and models are used. They lead to different results as shown below.

Keywords: proton; cross section; unitarity; spatial profile

1. Introduction

Traditionally, hadron collisions were classified according to our prejudices regarding the hadron structure. From the early days of Yukawa's prediction of pions, the spatial size of hadrons was ascribed to the pionic cloud surrounding their centers. The pion mass sets the scale of the size in the order of $1 \text{ fm} = 10^{-13} \text{ cm}$. Numerous experiments using different methods confirmed this estimate with values of the proton radius ranging from 0.84 fm to 0.88 fm. This 5% difference has been named the "proton radius puzzle". The different methods used in the various experiments could account for this discrepancy. Their sensitivity to central and peripheral regions may be different. Among the new experiments, I would like to mention recent results from the Jefferson laboratory [1] which reveal the internal QCD forces determining the pressure inside the proton. It happens that they are repulsive at the center (up to 0.6–0.7 fm) and attractive (strongest at about 0.9 fm) at the periphery ("an extremely high outward-directed pressure from the center of the proton, and a much lower and more extended inward-directed pressure near the proton's periphery"). It is also interesting that the lattice calculations showed that only 9% of "the gravitational strength" of a proton (its mass) is acquired from the Higgs mechanism. It is almost equally shared in three parts by kinetic energies of quarks and gluons and by their interactions. The three-quark content of protons is crucial for its static properties while the parton model is widely discussed for physics in collision. Surely, all of these details related to the proton substructure are important for their interaction.

Much less is known about the spatial extension of the interaction region of two colliding protons. The very external shell of a proton is usually described as formed by single pions as the easiest particle constituents. That is why the one pion exchange model was first proposed [2] for describing the peripheral interactions of hadrons. In general, both the size of the region and the strength of attenuation in different parts of it depend on the energy of colliding protons.

To get some insight into the spatial view of proton interactions, one must deal with the impact parameter representation of their scattering matrix. Its connection with experimental results on the transferred momentum dependence is established by the Fourier–Bessel transformation applied to the unitarity condition. Indeed, the proton sizes determine the spatial extension of their interaction region

and its evolution with an increase in energy. However, the tiny details of its shape appear to be closely related to the yet unknown properties of the elastic scattering amplitude. Therefore, we have to rely on “reasonable” assumptions and phenomenological models.

2. The Unitarity Condition

From the theoretical side, the most reliable information comes from the unitarity condition. The unitarity of the S -matrix $SS^+ = 1$ relates the amplitude of elastic scattering $f(s, t)$ to the amplitudes of inelastic processes M_n . In the s -channel, they are subject to the integral relation (for more details see, e.g., References [3,4]) which can be written symbolically as

$$\text{Im}f(s, t) = I_2(s, t) + g(s, t) = \int d\Phi_2 f f^* + \sum_n \int d\Phi_n M_n M_n^*. \quad (1)$$

The variables s and t are the squared energy and transferred momentum of colliding protons in the center of mass system $s = 4E^2 = 4(p^2 + m^2)$, $-t = 2p^2(1 - \cos \theta)$ at the scattering angle θ . The non-linear integral term represents the two-particle intermediate states of the incoming particles. The second term represents the shadowing contribution of inelastic processes to the imaginary part of the elastic scattering amplitude. Following Reference [5], it is called the overlap function. This terminology is ascribed to it because the integral there defines the overlap within the corresponding phase space $d\Phi_n$ between the matrix element M_n of the n -th inelastic channel and its conjugated counterpart with the collision axis of initial particles deflected by an angle θ in proton elastic scattering. It is positive at $\theta = 0$ but can change sign at $\theta \neq 0$ due to the relative phases of inelastic matrix elements M_n 's.

At $t = 0$ it leads to the optical theorem

$$\text{Im}f(s, 0) = \sigma_{tot} / 4\sqrt{\pi} \quad (2)$$

and to the general statement that the total cross section is the sum of cross sections of elastic and inelastic processes

$$\sigma_{tot} = \sigma_{el} + \sigma_{inel}, \quad (3)$$

i.e., that the total probability of all processes is equal to one.

To define the geometry of the collision, we must express all characteristics presented by the angle θ and the transferred momentum t in terms of the transverse distance between the trajectories of the centers of the colliding protons—namely the impact parameter, b . This is easily carried out using the Fourier–Bessel transform of the amplitude f which retranslates the momentum data to the corresponding transverse space features and is written as

$$i\Gamma(s, b) = \frac{1}{2\sqrt{\pi}} \int_0^\infty dt |f(s, t) J_0(b\sqrt{|t|})|. \quad (4)$$

The unitarity condition (1) stated in the b -representation reads

$$G(s, b) = 2\text{Re}\Gamma(s, b) - |\Gamma(s, b)|^2. \quad (5)$$

The left-hand side (the overlap function in the b -representation) describes the transverse impact parameter profile of inelastic collisions of protons. It is just the Fourier–Bessel transform of the overlap function g . It satisfies the inequalities $0 \leq G(s, b) \leq 1$ and determines how absorptive the interaction region is, depending on the impact parameter (with $G = 1$ for full absorption and $G = 0$ for complete transparency). The profile of elastic processes is determined by the subtrahend in Equation (5). If $G(s, b)$ is

integrated over all impact parameters, it leads to the cross section for inelastic processes. The terms on the right-hand side would produce the total cross section and the elastic cross section, correspondingly, as should be the case according to Equation (3). The overlap function is often discussed in relation with the opacity (or the eikonal phase) $\Omega(s, b)$ such that $G(s, b) = 1 - |\exp(-\Omega(s, b))|^2$. Full absorption corresponds to $\Omega = \infty$ and complete transparency to $\Omega = 0$.

Thus, it happens to be possible to study the space structure of the interaction region of colliding protons using information about their elastic scattering within the unitarity condition. The whole procedure is simplified because in the space representation, one gets an algebraic relation (5) between the elastic and inelastic contributions to the unitarity condition in place of the more complicated non-linear integral term I_2 in Equation (1).

The relation (5) is simplified if $\text{Im}\Gamma(s, b) \ll \text{Re}\Gamma(s, b)$, i.e., the integral contribution of the real part of the elastic scattering amplitude can be neglected as follows from the discussion below. Then,

$$G(s, b) = \zeta(s, b)(2 - \zeta(s, b)) = \text{Re}\Gamma(s, b)(2 - \text{Re}\Gamma(s, b)). \tag{6}$$

The absolute maximum of $G(s, b)$ is reached if $\text{Re}\Gamma(s, b) = 1$. At ISR energies, the maximum value at $b = 0$ is less than 1 (see Figure 1). It becomes close to 1 at 7 TeV.

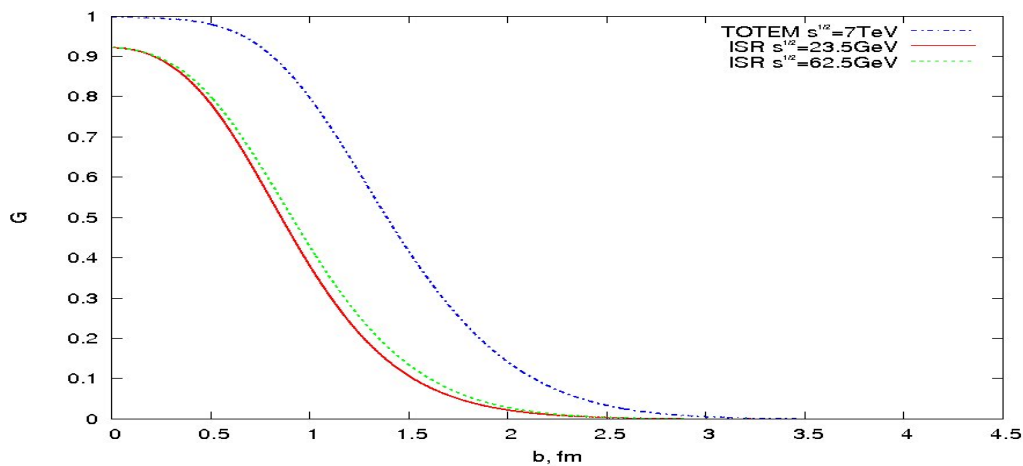


Figure 1. The proton profile $G(s, b)$ at 7 TeV (upper curve) [6] compared to those at ISR energies 23.5 GeV and 62.5 GeV [7] (the interpolation procedure of experimental data has been used). It was assumed in Reference [8] that the protons would become Blacker (less penetrable), Edgier, and Larger at higher energies (BEL-shape). We can see that both the blackness and the size of protons increase while its steepness at the edge varies very slowly.

3. How Different t -Regions Contribute to the Unitarity Condition

The main difficulty of this program is clearly seen from Equation (4). To calculate the contribution of different t -regions of the elastic scattering amplitude f to the unitarity condition (5), one must know, in principle, the behavior of its real and imaginary parts in the whole interval of the transferred momenta at a given energy s . However, from experiment, we know just its modulus given by the shape of the differential cross section $d\sigma/dt$ and the ratio ρ_0 of the real to imaginary parts at near forward scattering extracted from the interference of the nuclear and Coulomb amplitudes.

$$\frac{d\sigma}{dt} = |f(s, t)|^2 \equiv (\text{Re}f(s, t))^2 + (\text{Im}f(s, t))^2, \tag{7}$$

$$\rho_0 = \frac{\text{Re}f(s,0)}{\text{Im}f(s,0)}. \tag{8}$$

At $t = 0$, the imaginary part is positive according to the optical theorem (2). From experimental results at 7 TeV, one gets that the real part contributes less than 2% to $d\sigma/dt$ at $t = 0$, because the measured values $\rho_0 = \rho(t = 0) \approx 0.107 - 0.145$ [9–11] are so small. There are some theoretical considerations [12,13] supported by the phenomenological model [14] arguing that the real part should become even smaller and decrease fast within the diffraction cone crossing the abscissa axis. Therefrom, one concludes that the imaginary part dominates at low transferred momenta inside the diffraction cone. It was estimated in Reference [15] that the contribution to the proton profile from the real part can be neglected. The numerical estimates in Figures 2 and 3 below support this conclusion.

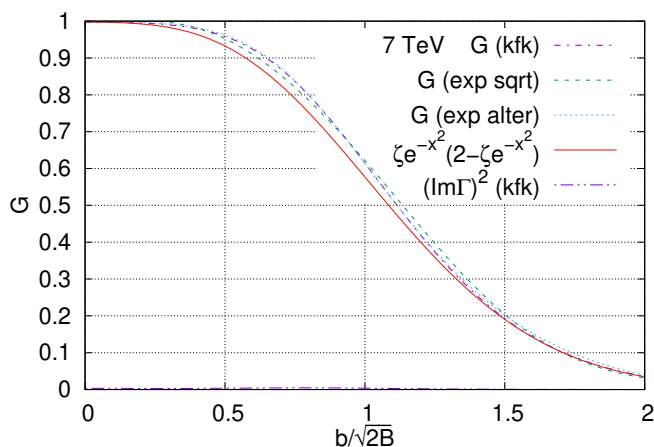


Figure 2. The transverse impact parameter profile (G) of inelastic collisions of protons at 7 TeV at different assumptions: kfk-model (dash-dotted line), $\text{Im}f(s, t) = \sqrt{d\sigma/dt}$ calculated from experimental data (dash line), $\text{Im}f(s, t) = \sqrt{d\sigma/dt}$ inside the diffraction cone and $\text{Im}f(s, t) = -\sqrt{d\sigma/dt}$ outside cone also calculated from experimental data (dotted line), shape $\zeta \exp(-x^2)(2 - \zeta \exp(-x^2))$ with $\zeta = 0.95058$ (solid line). Furthermore, the square of the imaginary part of Γ for kfk-model is shown by dash-double-dot line (very small contribution of the real part of the amplitude).

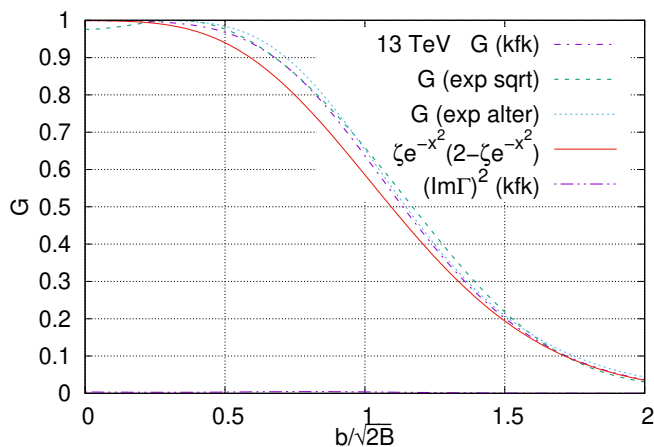


Figure 3. The same as Figure 2 but at 13 TeV and with $\zeta = 0.96906$.

The simplest approach to the problem consists in approximating the imaginary part by the $+\sqrt{d\sigma/dt}$. Doing that, one gets the evolution of the proton profile from ISR energies to 7 TeV at LHC as demonstrated in Figure 1 [16].

However, in general, both real and imaginary parts can be either positive or negative in different intervals of t . In any case, they are limited within $-\sqrt{d\sigma/dt}$ and $+\sqrt{d\sigma/dt}$ because their moduli cannot exceed $\sqrt{d\sigma/dt}$. The differential cross section is more than four orders of magnitude larger at the peak of the diffraction cone at $t = 0$ than after its dip, visible near $|t| \approx 0.5 \text{ GeV}^2$ at 7 TeV. It is reasonable to assume that the imaginary part becomes equal to 0 near the dip (which is filled in by a small real part there) and changes the sign at larger transferred momenta. Specifically, that happens in the model [14].

In what follows, we take into account the above information, neglect the real part of the amplitude, and adopt four approaches:

1. Use the experimental (spline interpolated) $+\sqrt{d\sigma/dt}$, i.e., $|f|$ everywhere in place of $\text{Im}f(s, t)$ in Equations (4) and (5).
2. Use the experimental $+\sqrt{d\sigma/dt}$ up to $|t_0|$ and $-\sqrt{d\sigma/dt}$ at $|t| > |t_0|$ in place of $\text{Im}f(s, t)$.
3. Use everywhere the exponential parameterization of the positive imaginary part to get the analytical expressions as described below.
4. Use the phenomenological model [14] which fits the experimental data in a wide energy interval and provides separately the real and imaginary parts of the amplitude.

Variants 1 and 2 correspond to two extreme possibilities of upper and lower estimates of the integral over the imaginary part. Variant 3 gives its value somewhat lower than variant 1 because of lower values of $d\sigma/dt$ at large transferred momenta. Model 4 leads to values between the two extremes, and moreover, shows that the contribution of the real part of the amplitude to the proton profile can really be neglected.

It is worthwhile to explain variant 3. The shape of the differential cross section in the diffraction cone can be approximated by the exponential behavior $d\sigma/dt \propto \exp Bt$. Therefore, it is possible to fit the imaginary part using the exponent which is twice as small. The role of the real part of the amplitude is negligibly small inside the cone. Neglecting it and extending the positive exponential shape of the imaginary part to all transferred momenta in an ad hoc fashion, one can calculate $G(s, b)$ analytically [16]. The most peculiar conclusion is that the inelastic profile for central collisions shows a dip $G(s, 0) < 1$ if the elastic cross section exceeds 1/4 of the total cross section. It is given by the formula [16]

$$G(s, 0) = 4x(1 - x). \quad (9)$$

Here, $x = 2\sigma_{el}/\sigma_{tot}$ so that $G(s, 0) < 1$ if $x > 1/2$. The ratio σ_{el}/σ_{tot} increases (surprisingly enough) from ISR to LHC energies and is near 1/4 at LHC. The maximum of $G(s, b) = 1$ shifts to positive values of b . Thus, the further increase of σ_{el}/σ_{tot} would imply the dip at $b = 0$. These results initiated the hypothesis on possible toroidal shape of the interaction region at higher energies.

The results of all four variants are shown in Figures 2 and 3 for 7 and 13 TeV [17].

It is clearly seen that the assumption about the universal positive imaginary part (variant 1) leads to the dip for central collisions at $b = 0$ (especially noticed at 13 TeV). The maximum $G(s, b_{max}) = 1$ moves to $b_{max} > 0$, i.e., the toroid-like shape is formed. The possibility of a dip at $b = 0$ was first considered in Reference [18]. The dip is less pronounced for variant 3 of the exponential parameterization because its tail at large transferred momenta is lower than for variant 1. If the imaginary part becomes negative at large transferred momenta (variants 2 and 4), no dip appears and the BEL-shape is recovered. That is specially demonstrated in Figure 4, which shows the region of central collisions at $b = 0$ at larger scales. The asymptotical predictions about the shape of the proton inelastic profiles are very sensitive to the integral contribution to those of the imaginary part of the amplitude. At the same time, the integral contribution of

the real part for model 4 is negligibly small (less than 0.01) as seen at the bottom of Figures 2 and 3. That confirms earlier estimates [15] and resolves the problem mentioned in References [19,20].

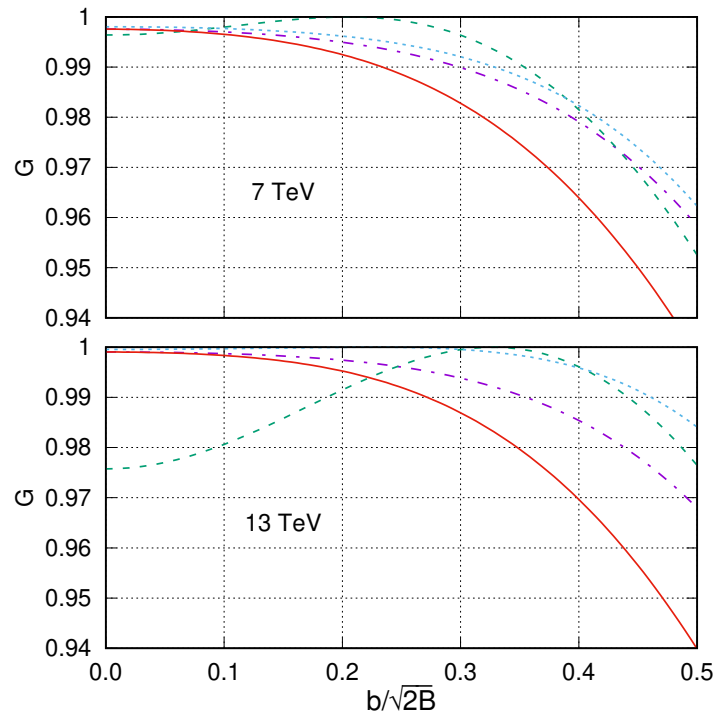


Figure 4. The area near $b = 0$ of Figures 2 and 3 in more detail.

A notable feature of $G(s, b)$ at ISR energies was noticed in Reference [7], where genuine experimental data were used. At the tail of large impact parameters (from 2 fm to 2.5 fm), a slight bump was observed. No bump was obtained in Reference [8], where some interpolation of the data was used. The results in References Figures 2 and 3 do not show any indication on such a bump. The corresponding values of $b = 2\sqrt{2B} \approx 2.5$ fm are similar to those in Reference [7].

It would be interesting to confront the predictions of variant 4 with new results obtainable with the help of the Levy-interpolation method [21]. Both of them predict the negative imaginary part at large transferred momenta. However, they differ in their approach to the problem. Model 4 [14] proposes the definite form of the elastic scattering amplitude inspired by QCD ideas. Its parameters are fitted by the existing experimental data and used for extrapolation to higher energies. The Levy-approach [21] is aimed at the direct interpolation of the differential cross section by the complete orthonormal set of complex functions suited for exponential and power-like dependence on transferred momenta revealed in experiment. The comparison of the results obtained in these two approaches on their predictions for the dip at $b = 0$ would be very instructive.

4. Conclusions

According to Equations (4) and (5), the spatial shape of the proton interaction region is determined by the integrals of the elastic scattering amplitude over all transferred momenta. The knowledge of its modulus obtainable from measurable differential cross sections is not enough to compute them. The prescription $\text{Im}f \approx |f| \approx +\sqrt{d\sigma/dt}$ leads to the toroidal shape at the highest LHC energies, while the

negative values of $\text{Im}f$ at large $|t|$ can recover the BEL-regime. No claim of the universality of such a mechanism is attempted here. It is just shown to work in variants 2 and 4, considered above.

Thus, the problem of the spatial shape of the proton interaction region cannot be solved rigorously unless the behavior (and, especially, the sign of the imaginary part) of the elastic scattering amplitude is known. Unfortunately, there does not currently seem to be a way of obtaining precise information about it. Once again, we repeat that one has to rely on “reasonable” speculations and phenomenological models confronted to a wide spectrum of experimental data. That is why the term “cul-de-sac” is used in the title of the paper.

Conflicts of Interest: The author declares no conflict of interest.

References

- Burkert, V.D.; Elouadrhiri, L.; Girod, F.X. The pressure distribution inside the proton. *Nature* **2018**, *557*, 396. [[CrossRef](#)]
- Dremin, I.M.; Chernavsky, D.S. Peripheral interactions of nucleons at 9-BeV. *JETP* **1960**, *11*, 167.
- Tanabashi, M.; Particle Data Group. Review of Particle Physics. *Phys. Rev. D* **2018**, *98*, 030001. [[CrossRef](#)]
- Dremin, I.M. Elastic scattering of hadrons. *Phys.-Uspekhi* **2013**, *56*, 3. [[CrossRef](#)]
- Van Hove, L. A phenomenological discussion of inelastic collisions at high energies. *Nuovo Cim.* **1963**, *28*, 798. [[CrossRef](#)]
- Dremin, I.M.; Nechitailo, V.A. Proton periphery activated by multiparticle dynamics. *Nucl. Phys. A* **2013**, *916*, 241. [[CrossRef](#)]
- Amaldi, U.; Schubert, K.R. Impact parameter interpretation of proton-proton scattering from a critical review of all ISR data. *Nucl. Phys. B* **1980**, *166*, 301. [[CrossRef](#)]
- Henzi, R.; Valin, P. Towards a blacker, edgier and larger proton. *Phys. Lett. B* **1983**, *132*, 443. [[CrossRef](#)]
- Antchev, G.; TOTEM Collab. Luminosity-independent measurement of the proton-proton total cross section at $\sqrt{s} = 8$ TeV. *Phys. Rev. Lett.* **2013**, *111*, 012001. [[CrossRef](#)]
- TOTEM Collaboration; Antchev, G.; Aspell, P.; Atanassov, I.; Avati, V.; Baechler, J.; Berardi, V.; Berretti, M.; Bossini, E.; Bottigli, U.; et al. Evidence for non-exponential elastic proton-proton differential cross-section at low $|t|$ and $\sqrt{s} = 8$ TeV by TOTEM, *Nucl. Phys. B* **2015**, *899*, 527. [[CrossRef](#)]
- Aaboud, M.; Aad, G.; Abbott, B.; Abdallah, J.; Abdinov, O.; Abeloos, B.; Aben, R.; AbouZeid, O.S.; Abraham, N.L.; Abramowicz, H.; et al. Measurement of the total cross section from elastic scattering in pp collisions at $\sqrt{s} = 8$ TeV with the ATLAS detector *Phys. Lett. B* **2016**, *761*, 158. [[CrossRef](#)]
- Martin, A. Asymptotic behaviour of the real part of the scattering amplitude at $t \neq 0$. *Lett. Nuovo Cim.* **1973**, *7*, 811. [[CrossRef](#)]
- Martin, A. A theorem on the real part of the high-energy scattering amplitude near the forward direction, *Phys. Lett. B* **1997**, *404*, 137. [[CrossRef](#)]
- Kohara, A.K.; Ferreira, E.; Kodama, T. pp elastic scattering at LHC energies. *Eur. Phys. J. C* **2014**, *74*, 3175. [[CrossRef](#)]
- Dremin, I.M.; Nechitailo, V.A.; White, S.N. Central and peripheral interactions of hadrons. *Eur. Phys. J. C* **2017**, *77*, 910. [[CrossRef](#)]
- Dremin, I.M. Interaction region of high energy protons. *Phys.-Uspekhi* **2015**, *58*, 61. [[CrossRef](#)]
- Dremin, I.M.; Nechitailo, V.A. Inelastic profiles of protons at 7 and 13 TeV. *Eur. Phys. J. C* **2018**, *78*, 913. [[CrossRef](#)]
- Troshin, S.M.; Tyurin, N.E. Beyond the black disk limit. *Phys. Lett. B* **1993**, *316*, 175. [[CrossRef](#)]
- Broniowski, W.; Arriola, E.R. Hollowness in pp scattering at the LHC. *Acta Phys. Polon. Suppl.* **2017**, *10*, 1203. [[CrossRef](#)]
- Broniowski, W.; Jenkovszky, L.; Arriola, E.R.; Szanyi, I. Hollowness in pp and $p\bar{p}$ scattering in a Regge model. *Phys. Rev. D* **2018**, *98*, 074012. [[CrossRef](#)]
- Csörgö, T.; Pasechnik, R.; Ster, A. Odderon and proton substructure from a model-independent Lévy imaging of elastic pp and $p\bar{p}$ collisions. *arXiv* **2019**, arXiv:1807.02897.

